Nucleic Acids Research, 2001, Vol. 29, No. 19 **3965–3974**

Nuclear antisense effects of neutral, anionic and cationic oligonucleotide analogs

Peter Sazani, Shin-Hong Kang, Martin A. Maier[1], Changfu Wei[1], Jennifer Dillman, James Summerton[2], Muthiah Manoharan[1] and Ryszard Kole*

Lineberger Comprehensive Cancer Center and Department of Pharmacology, CB# 7295, University of North Carolina at Chapel Hill, 102 Mason Farm Road, Chapel Hill, NC 27599, USA, [1]Department of Medicinal Chemistry, Isis Pharmaceuticals, Inc., Carlsbad, CA 92008, USA and [2]GeneTools, Corvallis, OR 97339, USA

Received June 26, 2001; Revised and Accepted August 6, 2001

ABSTRACT

The antisense activity of oligomers with 2′-*O*-methyl (2′-*O*-Me) phosphorothioate, 2′-*O*-methoxyethyl (2′-*O*-MOE) phosphorothioate, morpholino and peptide nucleic acid (PNA) backbones was investigated using a splicing assay in which the modified oligonucleotides blocked aberrant and restored correct splicing of modified enhanced green fluorescent protein (EGFP) precursor to mRNA (pre-mRNA), generating properly translated EGFP. In this approach, antisense activity of each oligomer was directly proportional to up-regulation of the EGFP reporter. This provided a positive, quantitative readout for sequence-specific antisense effects of the oligomers in the nuclei of individual cells. Nuclear localization of fluorescent labeled oligomers confirmed validity of the functional assay. The results showed that the free uptake and the antisense efficacy of neutral morpholino derivatives and cationic PNA were much higher than that of negatively charged 2′-*O*-Me and 2′-*O*-MOE congeners. The effects of the PNA oligomers were observed to be dependent on the number of L-lysine (Lys) residues at the C-terminus. The experiments suggest that the PNA containing Lys was taken up by a mechanism similar to that of cell-penetrating homeodomain proteins and that the Lys tail enhanced intracellular accumulation of PNA oligomer without affecting its ability to reach and hybridize to the target sequence.

INTRODUCTION

Antisense oligonucleotide-mediated down-regulation of genes that cause human diseases such as cancer and viral infections has been accomplished in cellular and animal models (1,2) and tested in clinical trials (3). Recently, an oligonucleotide has been approved as an antiviral drug (4). Most of these results have been obtained with oligodeoxynucleoside-phosphorothioates. Unfortunately, these oligonucleotides in cell culture and *in vivo* frequently exhibit non-antisense effects due to sequence-dependent as well as non-specific interactions with proteins (5,6). Chemical modifications such as C-5 propyne (7), substitutions at the 2′ position of the sugar (8), methylphosphonate oligonucleotides (9), peptide nucleic acid (PNA) (10), morpholino oligomers (11) (see Fig. 1B) and others (12) increase nuclease stability of the oligonucleotides and their affinity towards target RNA. Although modified oligonucleotides generally do not promote RNase H-mediated cleavage of the target RNA, this potential drawback in the application of oligonucleotides for down-regulation of gene activity is easily remedied by designing 'chimeric' or 'gapmer' oligonucleotides (1). More importantly, modified oligonucleotides are applicable not only for down-regulation but also for modification of gene expression (13). Their advantageous properties make modified oligonucleotides attractive for biological applications (14,15). Nevertheless, their antisense efficacy, uptake and/or pharmacodynamic properties are not yet optimal and further improvements in this regard are clearly desirable.

The main goal of this work was to characterize oligomers with modified backbones in terms of their uptake and antisense properties. To this end we have developed a unique test based on splicing of enhanced green fluorescent protein (EGFP) precursor to mRNA (pre-mRNA). The analysis of the EGFP fluorescence in individual cells after antisense treatment allows quantitation of sequence-specific, nuclear antisense function of oligonucleotides. It offers an alternative to assays based on down-regulation of targeted mRNAs or gene products, in which the background is high and distinguishing between non-specific and true antisense mechanisms or between cytoplasmic and nuclear effects of the oligonucleotides is not always easy. It also offers a standard platform by which non-RNase H-responsive synthetic oligonucleotides can be compared rapidly in a cell culture environment.

Application of the EGFP splicing assay identified marked differences in the antisense properties of modified anionic and neutral and cationic oligomers. PNA oligomers bearing positively charged lysine (Lys) tails showed a significantly enhanced cellular uptake and antisense activity surpassing their neutral and anionic counterparts. These results could

*To whom correspondence should be addressed. Tel: +1 919 966 1143; Fax: +1 919 966 3015; Email: kole@med.unc.edu

The authors wish it to be known that, in their opinion, the first two authors should be regarded as joint First Authors

Table 1. Sequence and backbone modification of the oligomers synthesized

Oligomer	Sequence 5′→3′	Target site	Backbone
1	GCT ATT ACC TTA ACC CAG	654	2′-*O*-Me, P = S
2	GCT ATT ACC TTA ACC CAG	654	2′-*O*-MOE, P = S
3	GCT ATT ACC TTA ACC CAG	654	Morpholino
4	H-GCT ATT ACC TTA ACC CAG-Lys-NH_2	654	PNA
5	H-GCT ATT ACC TTA ACC CAG-$(Lys)_2$-NH_2	654	PNA
6	H-GCT ATT ACC TTA ACC CAG-$(Lys)_4$-NH_2	654	PNA
7	CCT CTT ACC TCA GTT ACA	705	2′-*O*-Me, P = S
8	CCT CTT ACC TCA GTT ACA	705	2′-*O*-MOE, P = S
9	CCT CTT ACC TCA GTT ACA	705	Morpholino
10	H-CCT CTT ACC TCA GTT ACA-Lys-NH_2	705	PNA
11	H-CCT CTT ACC TCA GTT ACA-$(Lys)_2$-NH_2	705	PNA
12	H-CCT CTT ACC TCA GTT ACA-$(Lys)_4$-NH_2	705	PNA
13	H-GCT ACT ACA TTA AAC CAG-$(Lys)_4$-NH_2	654 3MM	PNA
14	H-CCA CTT ACC TCA GTT ACA-$(Lys)_4$-NH_2	705u	PNA

contribute to the development of the next generation of antisense oligomers as research tools and potent drugs.

MATERIALS AND METHODS

Plasmid and cell line construction

Insertion of the mutated human β-globin intron, IVS2-654 (16), at nucleotide 105 of EGFP cDNA was performed by a modified procedure of Jones (17,18). Briefly, vector pEGFP-N1 (Clontech, Palo Alto, CA) was linearized by PCR (one cycle at 95°C, 3 min; 30 cycles, 95°C, 1 min; 60°C, 1 min; 72°C, 5 min) with overlapping forward (5′-GGCGATGCCAC-CTACGGCAAGC-3′) and reverse (5′-GAGCGCACCATGT-TCTTCAAGG-3′) primers. PCR of plasmid IVS2-654 (19) with forward (5′-CGTGTCCGGCGAGGGCGAGGTGAGT-CTATGGGACCC-3′) and reverse (5′-GCTTGCCGTAGGT-GGCATCGCCCTGTGGGAGGAAGATAAG-3′) primers under the same conditions produced a linear IVS2-654 intron with the ends homologous to EGFP sequence. Transformation of Max DH5X cells (Life Technologies, Rockville, MD) with both DNA fragments led to homologous recombination and generation of the plasmid with IVS2-654 inserted in the coding sequence of EGFP.

HeLa S3 cells were transfected with 1 μg of IVS2-654 EGFP plasmid DNA by lipofection as suggested by the manufacturer (4 μl lipofectamine; Life Technologies). Stable cell lines were selected after 7–14 days in culture in minimum essential medium (MEM), supplemented with 5% fetal calf serum, 5% horse serum and 400 μg/ml G418.

Antisense oligonucleotides

Antisense oligomers were 18mers complementary to the β-globin intron 2 at the aberrant 5′ splice site around position 654. Control oligonucleotides were targeted downstream, around position 705. Both sequences were synthesized as 2′-*O*-methyl (2′-*O*-Me) phosphorothioate oligonucleotide (PTOs), 2′-*O*-methoxyethyl (2′-*O*-MOE) PTOs, morpholino and PNA oligomers (Table 1). 2′- *O*-Me oligonucleotides were purchased from TRI-Link, Inc. (San Diego, CA). 2′-*O*-MOE-modified PTOs were synthesized on an automated DNA synthesizer (Applied Biosystems, model 380B) using standard phosphoramidite chemistry. The oligonucleotides were analyzed by capillary gel electrophoresis and judged to be at least 90% full-length material. Morpholino oligonucleotides were synthesized as described elsewhere (20). PNA oligomers were synthesized in 10 μmol scale on a 433A Applied Biosystems Peptide Synthesizer using commercially available t-butyloxycarbonyl/benzyloxycarbonyl (Boc/Cbz)-protected monomers (Applied Biosystems) and synthesis protocols based on previously published procedures (21,22). The coupling efficiency was monitored by qualitative Kaisertest (23). The C-terminal Lys were introduced by using a resin pre-loaded with Boc-Lys(2-Cl-Z)-OH. Further Lys residues were introduced during solid-phase synthesis using the protocols for PNA synthesis. After cleavage and deprotection the PNA oligomers were purified by reversed-phase high performance liquid chromatography (RP-HPLC), analyzed by electrospray ionization mass spectrometry, lyophilized and stored at –20°C. Synthesis on a 10 μmol scale yielded >20 mg of PNA oligomer with a purity of >95% after RP-HPLC purification. Tetra methyl rhodamine (TAMRA), Texas Red and fluorescein (FITC) were used to label 2′-*O*-Me, 2′-*O*-MOE and morpholino oligomers, respectively.

Oligonucleotide delivery

HeLa cells expressing the IVS2-654 EGFP construct were maintained at below 80% confluence in S-MEM (Gibco-BRL) supplemented with 5% fetal calf serum, 5% horse serum and antibiotics. For scrape loading (24), cells were seeded 24 h before treatment in 24-well plates at ~10^5 cells per well in 0.5 ml of medium. For free uptake experiments, cells were

plated in 96-well plates at 8×10^3 cells per well in 150 µl of medium. For monolayers to be scrape-loaded the medium was aspirated and 0.5 ml of growth medium containing antisense oligonucleotides (concentrations as shown in figure legends) was applied. Cells were then scraped off the plate with a cell scraper (Costar, Corning, NY), re-plated in a fresh 24-well dish and assayed 24 h later. In free uptake experiments, growth medium was removed and replaced with 150 µl of fresh growth medium containing oligonucleotides. Cells were assayed 24 h later or as indicated in the figure legends.

RNA isolation and RT–PCR

Oligonucleotide-treated cells were lyzed in 0.8 ml of TRI-reagent (MRC, Cincinnati, OH) and total RNA was isolated. A 100 ng sample of RNA was used in RT–PCR with rTth enzyme (Perkin-Elmer, Branchburg, NJ) in the presence of 0.2 µCi of [α-^{32}P]dATP. Both procedures followed the manufacturer's protocols. The reverse transcription reaction was carried out at 70°C for 15 min followed by PCR: 1 cycle, 95°C, 3 min; 18 cycles, 95°C, 1 min; 65°C, 1 min. For EGFP mRNA amplification forward and reverse primers were 5′-CGTAAACGGCCACAAGTTCAGCG-3′ and 5′-GTGGTGCAGATGAACTTCAGGGTC-3′, respectively. The latter primer was used in the reverse transcription step. For β-globin, the forward and reverse primers spanned position 21–43 of exon 2 and position 6–28 of exon 3, respectively, as described in Sierakowska *et al.* (19). The PCR products were analyzed by electrophoresis on an 8% non-denaturing polyacrylamide gel. Gels were dried and autoradiographed with Kodak Biomax film at –80°C. Images were digitized by scanning with a Hewlett Packard scanner using Adobe Photoshop software.

Flow cytometry

Cells were trypsinized in 24- and 96-well plates with 200 and 100 µl 1× trypsin (Sigma, St Louis, MO), respectively, for 2 min at 37°C and resuspended in 1–2 ml of growth media. Approximately 10^4 cells from each sample were subjected to flow cytometry with a Becton-Dickinson FACScan (San Jose, CA) (flow rate = 100–200 cells/s). Dead or abnormal cells were omitted by gating of side versus forward scatter and histograms of green fluorescence intensity versus cell number were generated. The total mean fluorescence of the mock-treated controls was set to ~10^1 and the gate used for analysis of treated cells set to include 2.5% of most brightly fluorescent control cells as background. Consequently, treated samples could be analyzed in terms of a fluorescence index (FI). This number is derived by multiplying the percentage of cells scoring above the background threshold by the mean fluorescence intensity of that sub-population. Experimental conditions were established so that mock and untreated samples had a FI of 1.

Fluorescence microscopy

Cell culture medium was replaced with HBSS and bright field and UV images were taken using an inverted Olympus microscope (10× objective). Images were digitized using the Olympus digital imaging system and stored on a Power PC running Scion Image 1.62a software.

Confocal microscopy

HeLa EGFP-654 or HeLa cells not expressing EGFP-654 were cultured on 8-well slide wells at ~2×10^5 cells per well. Scrape loading was performed in a 24-well plate as described above, except that the cells were transferred to a new slide not a 24-well plate. For free uptake and cationic lipid transfections, treatment with the oligomer was performed in the slide well. Twenty-four hours after treatment, the cells were rinsed twice with PBS and fixed on the slide with 2% paraformaldehyde. Glass coverslips were mounted with Vecta-shield and sealed with nylon epoxy. Confocal images were taken within 48 h with an Olympus confocal microscope. For double staining, sequential scanning of each fluorophor was performed to prevent cross detection. Images were saved as TIFs and, when necessary, merged in Adobe Photoshop.

Toxicity assay

Approximately 10^4 cells/well were seeded in 96-well plates for 24 h. Media was then replaced with 100 µl media containing increasing amounts of free oligonucleotide. After 24 h, MTS (Promega, Madison, WI) was added directly to the culture wells as indicated by the manufacturer and the plates were incubated at 37°C for 2 h. Absorbance at 490 nm was measured and compared with that of mock-treated samples.

RESULTS

IVS2-654 EGFP reporter cell line

A C-to-T mutation at nucleotide 654 of the human β-globin intron-2 (IVS2-654) activates aberrant 5′ and 3′ splice sites that are preferably utilized during splicing, despite the presence of the normal, unaltered sites. The presence of this mutation in human β-globin gene interferes with correct expression of β-globin, causing thalassemia, a blood disorder (16). Previous reports from this laboratory have shown that antisense oligonucleotides hybridized to the aberrant β-globin 5′ splice site forced the splicing machinery to use the normal splice sites, resulting in correctly spliced β-globin mRNA. When the β-globin intron containing the mutation at position 654 is inserted at nucleotide 105 of EGFP cDNA, the spliced EGFP mRNA retains a portion of the globin intron, preventing correct translation of EGFP (Fig. 1A). Treatment of the cells expressing the IVS2-654 EGFP construct with active antisense oligonucleotide should restore proper splicing and translation of EGFP, providing a rapid and sensitive positive readout for antisense activity in the nuclei of the treated cells.

Transfection of the IVS2-654 EGFP HeLa cell line with 2′-*O*-Me-PTO oligonucleotide targeted to the aberrant 5′ splice site (ON-654, oligomer 1 in Table 1) and complexed with lipofectamine, a cationic lipid, resulted in up-regulation of the EGFP-IVS2-654 gene, detected as bright fluorescence (Fig. 2A). Fluorescent activated cell sorting (FACS) analysis (Fig. 2B) of treated cells showed an increase in the population of cells with fluorescence intensity ~15-fold higher than the baseline. The fluorescence did not increase in mock-treated cells or cells treated with a control oligonucleotide ON-705 (oligomer 7, Table 1) (Fig. 2B). Note that oligomer 7 hybridizes to a region of the intron 51 nt downstream from the IVS2-654 mutation and repairs splicing in another thalassemic mutant,

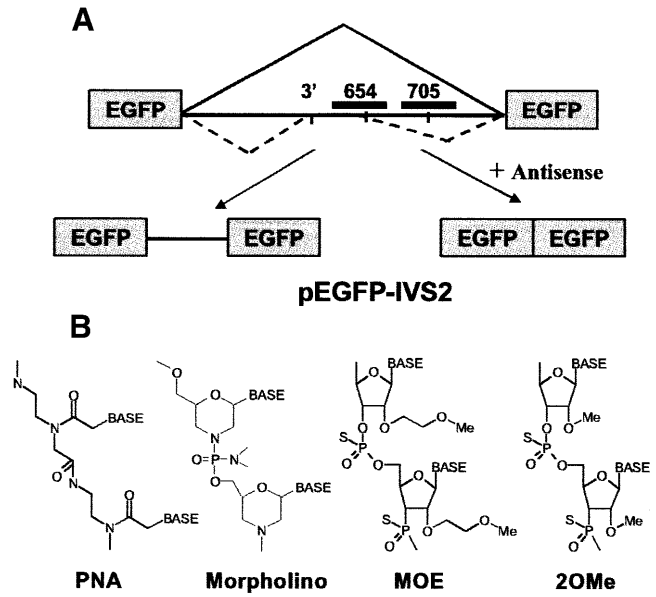

Figure 1. Splicing of IVS2-654 EGFP pre-mRNA. (**A**) The pre-mRNA contains a mutated intron 2 (IVS2-654) of human β-globin gene interrupting the EGFP cDNA sequence. The mutation at nucleotide 654 of the intron activates aberrant 5′ and 3′ splice sites leading to retention of the intron fragment in spliced mRNA. Antisense oligomers directed to position 654 prevent aberrant and restore correct splicing generating, as a result, the EGFP fluorescence signal. Control oligomers, targeting around position 705, have no effect. Boxes, EGFP coding sequence; horizontal line, intron; solid and dashed lines above and below intron, correct and aberrant splicing pathways; heavy bars above intron, antisense oligonucleotide. (**B**) Structures of oligonucleotides tested in this work.

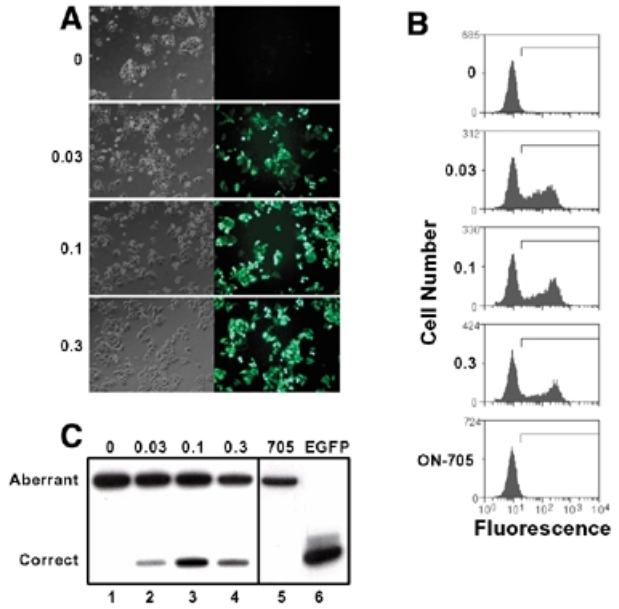

Figure 2. Restoration of EGFP expression by anti-654 oligomer 1 delivered with lipofectamine. Cells treated with increasing concentrations of the oligomer were analyzed by fluorescence microscopy (**A**) and FACS analysis (**B**). (A) Phase contrast (left) and UV (right) images are shown. (B) Histogram plots represent EGFP fluorescence intensity versus cell number. The line in each panel represents the gate set to include 2.5% of brightest fluorescent control cells as background. Concentrations (in μM) of oligomer 1 are indicated on the left. Control oligomer 7 is shown at the highest concentration tested (3 μM). The same designations are used in subsequent histograms. (**C**) RT–PCR of total RNA from cells treated with 1 (lanes 1–4). Oligomer concentration (μM) is indicated at the top. Lane 5, 0.1 μM control oligomer 7; lane 6, PCR product of EGFP cDNA as size marker. The upper and lower bands represent RT–PCR products of aberrantly and correctly spliced EGFP-654 mRNA, respectively.

IVS2-705 (25). It is also partially complementary to the IVS2-654 splice site, with only six mismatches if G–U or G–T base pairing is taken into account. Thus, oligomer 7 provides a stringent control for sequence specificity of the antisense effects of ON-654. The use of oligonucleotides against constructs containing the IVS2-654 sequence and evidence of sequence specificity and antisense mechanism of action has also been reported previously (25–27).

To confirm that the induced, green fluorescence was due to correction in splicing of the EGFP pre-mRNA, total cellular RNA was analyzed by RT–PCR (Fig. 2C). In cells treated with oligomer 1, a shorter band representing correctly spliced EGFP mRNA (Fig. 2C, lane 6) appeared in addition to a longer product of aberrant splicing (Fig. 2C, lanes 2–4); maximal correction occurred at 0.1 μM oligonucleotide. Treatment of the cells with the control oligomer 7 had no effect (Fig. 2C, lane 5). As, in this experiment, the concentration of lipofectamine was held constant while the oligonucleotide concentration was increased, the lower activity of oligomer 1 at 0.3 μM is due to inappropriate lipofectamine–oligonucleotide ratio (Fig. 2C, lane 4). The results indicate that in a subpopulation of treated cells, oligomer 1 crossed the cell membrane, entered the nucleus and in a sequence-specific manner shifted splicing from aberrant to correct in the EGFP system. Thus, the RT–PCR analysis validated the use of fluorescence assay and confirmed that the oligomers acted by affecting splice site choice. Similar results were obtained with the 2′-*O*-MOE derivative, oligomer 2 and its control oligomer 8 (see Fig. 6).

Free uptake of 2′-*O*-Me, 2′-*O*-MOE, morpholino and PNA oligomers

To elucidate the influence of the backbone modification on the cellular uptake and antisense properties of different oligonucleotide analogs, the latter were tested in the EGFP assay. Negatively charged (2′-*O*-Me and 2′-*O*-MOE) oligomers and neutral or cationic morpholino and PNA oligomers targeted to the 654 splice site were evaluated in cells treated in the absence of transfection reagents (Fig. 3). Results are reported as the FI. The index takes into account the percentage of fluorescent cells in the sample and the intensity of their fluorescence (see Materials and Methods). For example, for 3 μM morpholino and PNA analogs (oligomers 3 and 4), the FI increased from a background of 1 to ~65 and 80, respectively (see inset numbers in Fig. 3). The percentage of cells exhibiting fluorescence above background increased to 55 and 70% of the cell population. In contrast, with the same concentration of negatively charged 2′-*O*-Me and 2′-*O*-MOE oligonucleotides (oligomers 1 and 2), FIs of only 5 and 20 were observed, respectively; the percentage of cells that scored above background was only 8% for 2′-*O*-Me and 19% for 2′-*O*-MOE. Non-linear regression

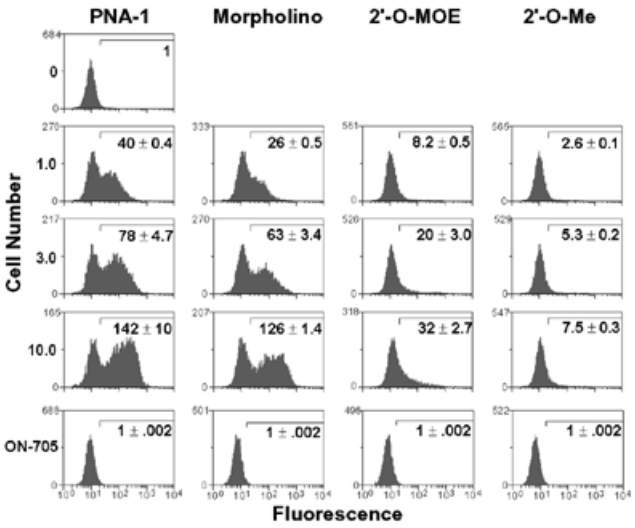

Figure 3. Free uptake of oligomers 1–4 by EGFP-654 HeLa cells. Cells were incubated in growth media containing increasing concentration (μM, shown on left) of anti-654 oligomers 1–4 or 25 μM control oligomers 7–10 (ON-705). Top panel represents mock-treated cells in the absence of oligomers and, therefore, applies to all four backbones. Inset numbers represent the average FI of treated cells (n = 3). FI provides the measure of antisense efficacy and efficiency of oligomer delivery (see Materials and Methods). Error represents standard deviation.

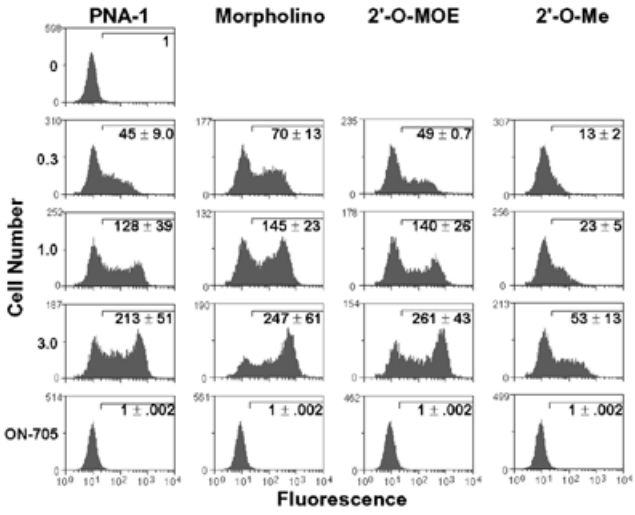

Figure 4. Scrape loading of oligomers 1–4 into EGFP-654 HeLa cells. Cells were scrape-loaded with increasing concentrations of oligomers 1–4 (μM, shown on left) or 3 μM control oligomers 7–10. Inset numbers are as described in the legend to Figure 3.

Table 2. Quantitation of FACS analysis

Oligomer	Scrape		Free uptake	
	FI_{max}	EC_{50} (μM)	FI_{max}	EC_{50} (μM)
1	101 ± 14	2.9 ± 0.7	9 ± 1	2.6 ± 0.5
2	477 ± 15	2.5 ± 0.1	45 ± 4	3.9 ± 0.8
3	361 ± 13	1.4 ± 0.1	220 ± 6	7.5 ± 0.4
4	337 ± 12	1.7 ± 0.1	208 ± 12	4.7 ± 0.6
5	291 ± 19	1.2 ± 0.2	217 ± 9	3.3 ± 0.4
6	314 ± 21	1.5 ± 0.3	221 ± 4	2.1 ± 0.2

Non-linear regression analysis of the data from Figures 3, 4, 5A and C was performed using GraphPad Prizm software (San Diego, CA). FI_{max} is expressed in arbitrary units and EC_{50} is expressed in μM (±SEM).

analysis of the dose response data revealed a theoretical limit of the FI specific for each backbone and delivery method. This allowed us to characterize each oligomer/delivery combination in terms of an EC_{50} and a maximal FI (FI_{max}). The results are summarized in Table 2.

The effects of all four oligonucleotide analogs are due to hybridization of the antisense oligomer to the target site on pre-mRNA, as mock-treated cells and cells treated with control oligomers targeted against the 705 site showed only background fluorescence (Fig. 3, top and bottom panels). The sequence specificity was further confirmed by the fact that the oligomers targeted to the 654 site were inactive against cells expressing an EGFP construct with an aberrant 5′ splice site located at nucleotide 705 of the intron (data not shown). Overall, the results suggest that neutral and cationic morpholino and PNA oligomers more readily cross the cell membrane barrier and gain access to the nucleus than their anionic counterparts (2′-*O*-MOE and 2′-*O*-Me).

To assess the contribution of uptake through the cell membrane on the antisense efficacy of the four oligonucleotide-analogs, the oligomers were delivered to cells by scrape loading. Scrape loading facilitates entry of large molecules into cells as a result of mechanical damage to the cell membrane (24). By this method, PNA, morpholino and 2′-*O*-MOE oligomers 4, 3 and 2, respectively, led to a dose-dependent and very similar increase in the population of fluorescent cells, while the effects were less pronounced for the 2′-*O*-Me oligomer 1 (Fig. 4). This suggests that the observed differences in the antisense efficacy of oligomers in the absence of transfection reagents (Fig. 3) are predominantly a function of their ability to cross the cell membrane (see also below).

Nuclear accumulation of effective oligomers

As the oligonucleotide-induced EGFP fluorescence was due to correction of splicing of EGFP pre-mRNA, it was expected to correlate with increased nuclear accumulation of the oligonucleotides. The reasons for poor effectiveness of free 2′-*O*-Me and 2′-*O*-MOE were less clear. We addressed these issues by using TAMRA-labeled 2′-*O*-Me, Texas Red-labeled 2′-*O*-MOE and FITC-labeled morpholino oligomers. Fluorescent-labeled PNA derivatives were not available. Because FITC fluorescence is difficult to distinguish from that of EGFP, the oligonucleotides were delivered to wild-type HeLa cells devoid of the EGFP-654 gene.

Free uptake of either 2′-*O*-Me or 2′-*O*-MOE oligomers did not lead to their significant accumulation in the nucleus. Rather, punctate or diffuse staining of the cytoplasmic space was seen. In contrast, morpholino oligomers concentrated in and brightly illuminated the nuclei and to a lesser extent the cytoplasm of the treated cells (Fig. 5, left panels). Thus, the nuclear accumulation of the oligomers mirrored their antisense

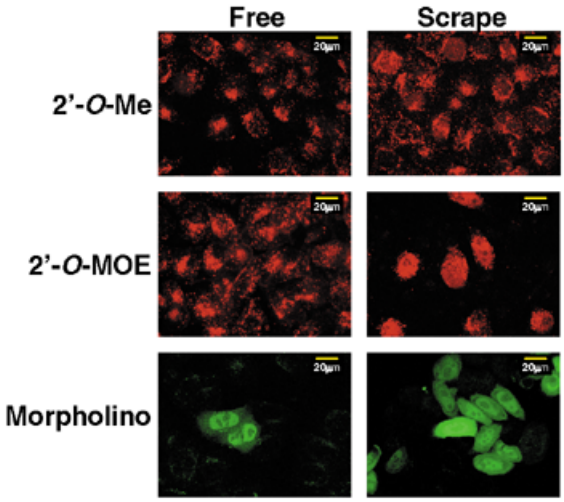

Figure 5. Cellular localization of modified oligomers. HeLa cells lacking the EGFP-654 gene were treated with fluorescent TAMRA 2′-*O*-Me, Texas Red 2′-*O*-MOE and FITC morpholino oligomers at 1 (scrape loading) and 3 μM (free uptake) concentrations. Cells were cultured and treated on an 8-well slide and fixed with 2% paraformaldehyde after treatment directly to the slide. Images were taken with an Olympus confocal microscope.

activity in the EGFP-654 cells (Fig. 3). Similarly, strong nuclear localization of the oligomers was detected in cells scrape-loaded with either 2′-*O*-MOE or morpholino oligomers (Fig. 5, right panels), which elicited high levels of EGFP production in the EGFP-654 cell line (Fig. 4). Scrape-loaded 2′-*O*-Me oligomers resulted in poorer nuclear staining (Fig. 5, top right panel) and EGFP production (Fig. 4) further supporting the interpretation that nuclear accumulation of the oligomer is required for antisense activity.

As expected from the EGFP results (Fig. 4), the three derivatives, particularly the 2′-*O*-MOE oligomer, accumulated at higher nuclear levels under scrape-loading conditions. Thus, like other physical methods of delivery, such as microinjection or syringe loading (28), scrape loading allows the extracellular contents to by-pass the membrane, enter the intracellular space and migrate to the nucleus.

We took advantage of the fact that in confocal microscopy the red fluorescence of labeled 2′-*O*-Me and 2′-*O*-MOE can be easily distinguished from the EGFP signal to directly compare if high nuclear accumulation results in high activity in our assay (Fig. 6). As expected, in cells scrape-loaded with 2′-*O*-Me and 2′-*O*-MOE oligomers, only those with nuclear staining produced EGFP. When a cationic lipid was used as a carrier, high nuclear levels of both oligomers caused concomitant increase in EGFP production (Fig. 6, right). Note that FITC-labeled morpholino oligomers could not be tested on EGFP-654 cells because they fluoresce at the same wavelength as EGFP.

It is notable that, in spite of a rather similar chemistry of 2′-*O*-Me and 2′-*O*-MOE oligonucleotides, their antisense effects and nuclear accumulation appear very different except when delivered with a cationic lipid (see Discussion).

Antisense efficacy of PNA is influenced by the number of attached lysine residues

To further examine the effects of the backbones on the antisense properties of the oligomers, we compared antisense PNAs modified with one, two and four positively charged Lys residues at the C-terminus (PNA-1, -2 and -4; oligomers 4, 5 and 6 in Table 1). The significant, dose-dependent increases in fluorescence of the cells treated with the Lys-modified PNAs are apparent from Figure 7A and B. Quantitative analysis of FACS data from several experiments (Table 2) clearly demonstrates that the PNA containing four Lys residues (PNA-4, oligomer 6) was the most effective in generating EGFP fluorescence in treated cells; its EC_{50} (2.1 μM) was almost 2.5 times lower than that of PNA-1 (4.7 μM, oligomer 4). The FI_{max} was comparable with each of the modified PNAs suggesting that at high concentrations all three derivatives are highly effective. For all three derivatives ~70% of the cell

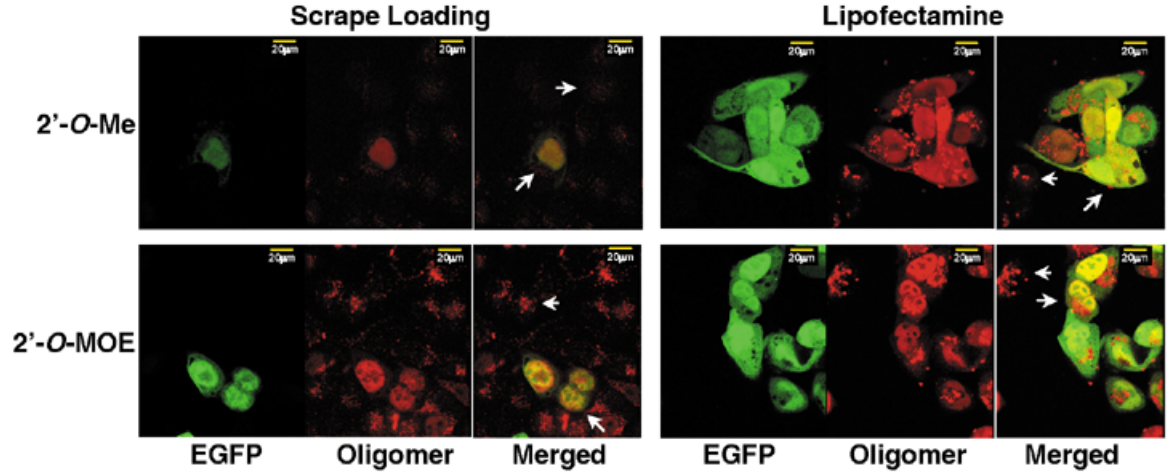

Figure 6. Treatment of EGFP-654 cells with labeled oligomers. Fluorescently labeled 2′-*O*-Me (TAMRA) or 2′-*O*-MOE (Texas Red) oligomers were used to treat EGFP-654 cells either by scrape loading (1 μM) or by cationic lipid delivery (0.03 μM). Images were generated by sequential excitement of the oligomer label followed by EGFP. EGFP (green) and oligomer (red) images were merged, with co-localization appearing as shades of yellow.

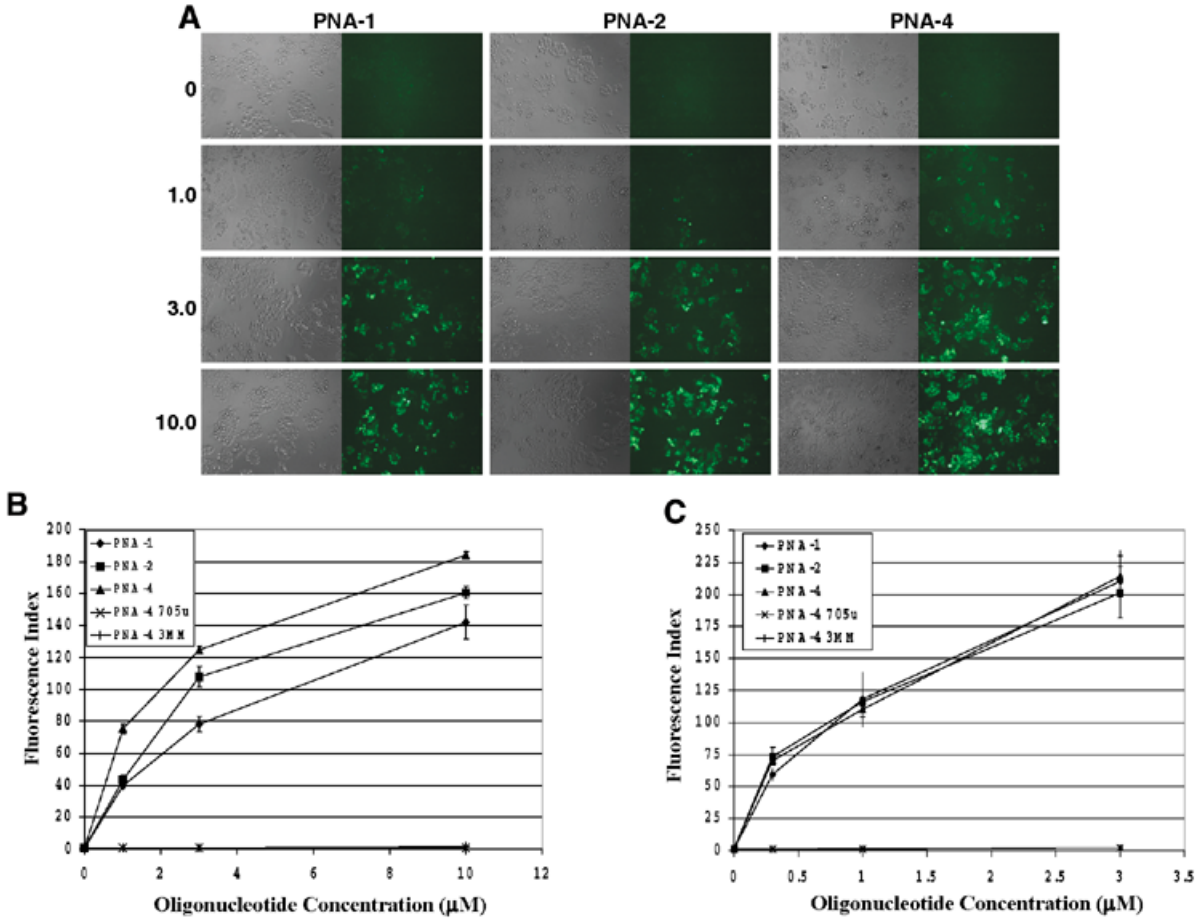

Figure 7. Effect of Lys residues on the antisense efficacy of PNA oligomers. Free uptake of PNA oligomers 4, 5 and 6 with one, two and four Lys residues at the C-terminus, respectively, were analyzed by fluorescence microscopy (**A**). Quantitation of FACS data (FI; average of at least three experiments) from free uptake (**B**) and scrape-loading (**C**) experiments for oligomers 4, 5, 6, 13 and 14. Oligomer 13 has three mismatches (PNA-4 3MM) with the 654 sequences. Oligomer 14 is targeted to the region of IVS2 52 nt downstream (PNA-4 705u). Error bars show standard deviation (n = 3).

population became fluorescent suggesting that the Lys tail increased the actual concentration of the oligonucleotide within the cells rather than the number of transfected cells.

In contrast, no difference was observed in the EC_{50}, FI_{max} or the FIs in cells scrape-loaded with PNA-1, -2 and -4 at any tested concentration (Fig. 7C and Table 2). These results indicate that the Lys residues attached to the C-terminus of PNA oligomers did not increase their affinity to the target sequence nor influence the nuclear translocation process. Rather, the observed Lys-dependent enhancement of the antisense efficacy in free uptake experiments must have resulted from improved transport of the PNA molecules through the cell membrane or from an enhanced release from the endosomes. Although direct measurement of nuclear accumulation was not possible because of the lack fluorescent labeled PNAs, the above data along with data from the labeled oligomers indicate that the added Lys increased cellular uptake and thus nuclear accumulation of the free PNA derivatives.

Uptake of PNA-4

To gain an understanding of how the $(Lys)_4$ tail increased the antisense efficacy of PNA oligomers, cells were incubated with PNA-4 (oligomer 6) for 3 h at a 10 μM concentration and at either 4 or 37°C. For comparison, morpholino (oligomer 3) and 2′-*O*-MOE (oligomer 2) derivatives were also tested (Fig. 8A). After treatment, the oligomers were removed by rinsing the cells with culture media and the cells were allowed to recover at 37°C for 20 h. Incubation at 4°C lowered the overall intensity of fluorescence of the cells treated with any nucleotide (data not shown); however, only in cultures treated with PNA-4 did the number of fluorescent cells remain the same, regardless of the incubation temperature. These results strongly suggest that the mechanism of uptake of positively charged PNA derivative is different from those of neutral morpholino and negative 2′-*O*-MOE analogs (see Discussion)

A time course experiment with oligomers 1, 2, 3 and 6 at 1 μM concentration was carried out. All oligomers exhibited a time-dependent increase in EGFP fluorescence (Fig. 8A), but the rate for the positively charged PNA-4 was higher than those observed for the other oligomers with neutral or anionic backbones. Between 12 and 48 h of incubation with PNA-4 (oligomer 6) the FI increased 20-fold, while only a 10-fold increase was observed for both the morpholino and 2′-*O*-MOE derivatives 3 and 2, respectively. (Note: the FI value for 3 is approximately nine times higher that the FI value of 2 at 12 h.) This further suggests that the uptake properties of PNA-4 are

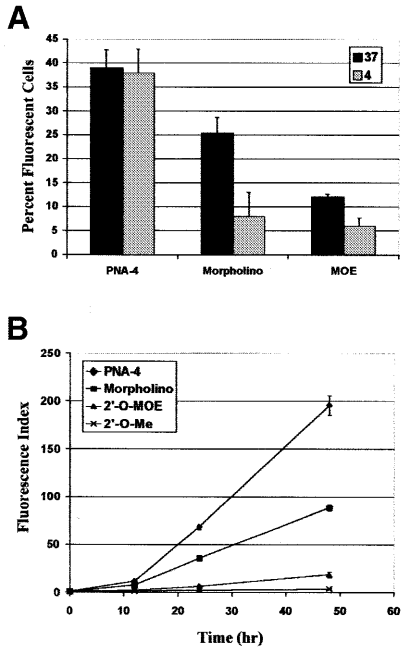

Figure 8. Temperature and time dependence of antisense effects. (**A**) Temperature dependence of uptake. Cells plated in 96-wells were pre-incubated at 4 or 37°C for 30 min before application of media containing 10 μM PNA-4, morpholino and 2′-*O*-MOE oligomers (6, 3 and 1) indicated below the diagram. Free uptake was allowed to occur at either 4 or 37°C for 3 h; oligonucleotides were removed by replacing the culture medium and the cells were allowed to recover at 37°C for 20 h. FACS data from three experiments were quantified. Bars indicate the percentage of cells with fluorescence intensity above background. Error bars show standard deviation (n = 3). (**B**) Time course of free uptake. Cells were incubated with oligomers 1, 2, 3 and 6 at a concentration of 1 μM for 12–48 h and analyzed by FACS. FI of samples were tabulated and expressed as an increase over mock-treated samples versus time of incubation. Error bars show standard deviation (n = 3).

unique compared with those shared by neutral morpholino and negatively charged PTOs.

Positively charged oligomers are not toxic and sequence specific

Toxicity of oligonucleotide analogs, especially of cationic derivatives, in free uptake experiments was of concern since high concentrations of up to 10 μM were used. However, the growth rates of mock-treated cells and cells treated with the antisense oligomers were comparable, indicating that these compounds do not cause cytotoxicity at the concentrations tested. In addition, toxicity of PNA-4 was analyzed by MTS assay at a 10 μM concentration. No toxicity was observed despite the presence of the $(Lys)_4$ tail at the C-terminus of the oligomer (data not shown). Normal cell growth rate and lack of toxicity suggest that PNA-4 and the other tested oligomers do not significantly interfere with splicing of non-target RNAs or with other cellular processes, further confirming the sequence specificity of the observed antisense effects.

The sequence specificity of the PNA-4 oligomer was tested using a three-mismatch control (oligomer 13) and an oligomer directed to a region of IVS-2 50 bases downstream (oligomer 14). These oligomers had negligible effects on splicing at any concentration tested (Fig. 7B and C).

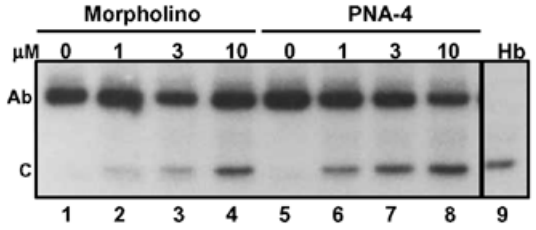

Figure 9. Correction of splicing of the β-globin IVS2-654 pre-mRNA. HeLa cells stably expressing human β-globin IVS2-654 gene were treated with the indicated concentration of morpholino (oligomer 3) or PNA-4 (oligomer 6) derivatives for 18 h. Correction of splicing was detected by RT–PCR using β-globin-specific primers as described in Materials and Methods and in the legend to Figure 2C. Ab, aberrantly spliced; C, correctly spliced. The lane marked Hb represents RT–PCR of total RNA from the blood of a non-thalassemic volunteer.

Application of the EGFP-654 reporter assay

The PNA-4 (oligomer 6) and morpholino (oligomer 3) oligomers were used in the previously developed cellular model of β-thalassemia (19,25) to test if the results obtained in the EGFP-654 assay are relevant to models of clinical disease. Treatment of the cells with either oligonucleotide in the absence of transfection reagents led to restoration of correct splicing of the IVS2-654 human β-globin pre-mRNA (Fig. 9). Importantly, analysis of RT–PCR results shown in Figure 9 indicates that oligomer 6 was approximately four times more effective than oligomer 3 at correcting pre-mRNA splicing (compare lanes 2–3 versus 6–8). These results are in qualitative and quantitative agreement with those obtained in the EGFP based assay. They therefore confirm the utility of the latter system in predicting effectiveness of different oligonucleotide chemistries in modification of splicing pathways.

DISCUSSION

The antisense assay based on modification of splicing and EGFP expression has a number of significant advantages. The signal is positive, easily detectable and of high sensitivity. The shift in splicing ascertains sequence specificity and because splicing takes place in the nucleus, the observed effects must result from nuclear antisense activity of oligonucleotides. The results from the EGFP assay are directly applicable to other splicing systems (Fig. 9). Finally, and perhaps most importantly, signal is detected in individual cells. The importance of the last feature is exemplified by our findings concerning the differences in the uptake of PNA-4 (oligomer 6) compared with the other oligonucleotide analogs. The assay simultaneously assesses the antisense effect and the distribution of the oligomers in treated cultures. This is accomplished without fluorescent labeling of the oligonucleotide, but it is equally reflective of its nuclear accumulation.

The EGFP signal is generated only if pre-mRNA splicing, a nuclear process, is shifted from aberrant to correct. Thus, the effects of the antisense oligomers described here are exclusively nuclear. Other studies have shown that increased antisense effects were detected only if oligonucleotides were delivered to the nuclei by cationic lipids, but not if the oligonucleotides remained in the endosomal compartment in the

cytoplasm (29). Furthermore, oligonucleotides targeted to spliced mRNA had unexpected effects on splicing events (30). Sequences important for splicing of pre-mRNAs have proven excellent targets for the antisense approach (26,31–34). These studies all provide compelling evidence that the nucleus represents a major site of antisense oligonucleotide activity.

The EGFP-IVS2-654 reporter assay revealed several important properties of oligonucleotide analogs with modified backbones. When oligomers were scrape-loaded into cells, PNA, morpholino and 2′-*O*-MOE oligomers exhibited high and similar FI_{max} values (Table 2). Markedly lower FI_{max} values were obtained with the 2′-*O*-Me analog. There are two possible reasons for the latter observation: (i) the 2′-*O*-Me oligomer is inherently unable to efficiently enter the nucleus either free or in scrape-loaded cells, or (ii) a lower resistance to nucleases leads to degradation of this oligomer in serum or in cells without the protection of a cationic lipid. The first is unlikely as widely varying chemistries act similarly under these conditions, one of which (2′-*O*-MOE) differs from 2′-*O*-Me by only a few atoms at the 2′ position. The second possibility is also supported by previous observations (8). Interestingly, the EC_{50} for both 2′-*O*-Me and 2′-*O*-MOE PTOs was up to 2-fold higher than those of the neutral and positive oligomers. This may be a consequence of the lower affinity and slower on-rate of hybridization to the RNA target caused by charge repulsion of the anionic backbones.

In contrast, free uptake of the oligonucleotide analogs resulted in antisense effects that were clearly dependent on the charge of the backbone. FI_{max} values for the neutral and positively charged analogs were similar and much higher than those observed for the negatively charged oligomers 1 and 2. Similarly, labeled neutral oligomers localized to the nucleus more efficiently by free uptake than their charged counterparts (Fig. 5). The neutral and positively charged analogs rank $6 < 5 < 4 < 3$ from the lowest to the highest EC_{50} values with an almost 4-fold increase from PNA-4 (oligomer 6) to the morpholino oligomer 3**.** This difference in antisense activity between PNA-4 and morpholino analogs was also seen in the context of the clinically relevant β-globin gene with a thalassemic defect (Fig. 9). For the PNA series, change in length of the Lys tail from one to four residues enhanced the efficacy by a factor of more than two, leading to a conclusion that the free uptake of oligomers was significantly influenced by the net charge of the backbone. The free uptake FI_{max} values for the negatively charged oligomers 1 and 2 were significantly lower than those of the neutral and positively charged oligomers (Table 2). This makes comparison of their EC_{50} values to those of the neutral and positively charged oligomers irrelevant, as overall efficacy of the negatively charged oligomers was so low.

Uptake of anionic and neutral oligomers was temperature-dependent (Fig. 8A), suggesting an endocytotic event. In contrast, the uptake of the positively charged PNA-4 was temperature-independent suggesting that a receptor- and transporter-independent mechanism is involved in the penetration of the cellular membrane. Several reports show that addition of peptides of 16–35 amino acid residues with sequences derived from HIV TAT or *Drosophila* penetratin to oligonucleotides facilitated transport of the conjugates through cell membrane (35–37). The studies reveal that this transport is independent of energy, chirality and, to some extent, sequence. The common characteristic of the conjugates is the highly basic nature of the amino acids. Our study suggests that short, basic sequences, such as the four-Lys chain, are sufficient to enhance cellular penetration of conjugated PNAs. In comparison with conjugates with long peptides this modification contributes to a more facile and less expensive oligomer synthesis, an important consideration in antisense applications.

Although the EC_{50} of PNA-4 in free uptake is still relatively high, the results suggest ways of improving the properties of antisense oligonucleotides. Optimization of cationic tails, using residues other than Lys, in combination with neutral or anionic backbones, may result in even better results. Furthermore, rational development of short sequences containing other key elements of the homeodomain peptides such as tryptophan (38) may further improve cellular delivery of PNA–peptide oligomers.

The methods described in this work for the evaluation of antisense oligomers in cultured cells could also be applicable *in vivo* with the IVS654-EGFP or similar constructs expressed in transgenic animals. In view of the fact that penetrating peptides appear to be capable of reaching all tissues including the brain (35), PNA–peptide conjugates are promising candidates for the next generation of antisense therapeutics.

ACKNOWLEDGEMENTS

We thank Dr C. F. Bennett for critical reading of this manuscript and Elizabeth Smith for technical assistance. This work was supported by NIH grant PO1-59299 to R.K.

REFERENCES

1. Crooke,S.T. (2000) Progress in antisense technology: the end of the beginning. *Methods Enzymol.*, **313**, 3–45.
2. Agrawal,S. and Zhao,Q. (1998) Antisense therapeutics. *Curr. Opin. Chem. Biol.*, **2**, 519–528.
3. Flanagan,W.M. (1998) Antisense comes of age. *Cancer Metastasis Rev.*, **17**, 169–176.
4. Crooke,S.T. (1998) Vitravene—another piece in the mosaic. *Antisense Nucleic Acid Drug Dev.*, **8**, vii–viii.
5. Stein,C.A. (1999) Keeping the biotechnology of antisense in context. *Nat. Biotechnol.*, **17**, 209.
6. Neckers,L. and Iyer,K. (1998) Nonantisense effects of antisense oligonucleotides. In Stein,C. and Krieg,A. (eds), *Applied Antisense Oligonucleotide Technology*. Wiley Liss Inc., New York, NY, pp. 147–159.
7. Wagner,R.W., Matteucci,M.D., Lewis,J.G., Gutierrez,A.J., Moulds,C. and Froehler,B.C. (1993) Antisense gene inhibition by oligonucleotides containing C-5 propyne pyrimidines. *Science*, **260**, 1510–1513.
8. Manoharan,M. (1999) 2′-carbohydrate modifications in antisense oligonucleotide therapy: importance of conformation, configuration and conjugation. *Biochim. Biophys. Acta*, **1489**, 117–130.
9. Jager,A. and Engels,J. (1984) Synthesis of deoxynucleoside methylphosphonates via phosphonamidite approach. *Tetrahedron Lett.*, **25**, 1437–1440.
10. Nielsen,P.E., Egholm,M., Berg,R.H. and Buchardt,O. (1991) Sequence-selective recognition of DNA by strand displacement with a thymine-substituted polyamide. *Science*, **254**, 1497–1500.
11. Seeberger,P. and Caruthers,M. (1998) Modified oligodeoxynucleotides as antisense therapeutics. In Stein,C. and Krieg,A. (eds), *Applied Antisense Oligonucleotide Technology*. Wiley Liss Inc., New York, NY, pp. 51–71.
12. Altmann,K., Cuenoud,B. and Von Matt,P. (1998) Novel chemistry. In Stein,C. and Krieg,A. (eds), *Applied Antisense Oligonucleotide Technology*. Wiley Liss Inc., New York, NY, pp. 73–107.
13. Kole,R. and Sazani,P. (2001) Antisense effects in the cell nucleus: modification of splicing. *Curr. Opin. Mol. Therap.*, **3**, 229–234.

14. Zhang,H., Cook,J., Nickel,J., Yu,R., Stecker,K., Myers,K. and Dean,N.M. (2000) Reduction of liver Fas expression by an antisense oligonucleotide protects mice from fulminant hepatitis. *Nat. Biotechnol.*, **18**, 862–867.
15. Summerton,J. (1999) Morpholino antisense oligomers: the case for an RNase H-independent structural type. *Biochim. Biophys. Acta*, **1489**, 141–158.
16. Schwartz,E. and Benz,E. (1995) Thalassemia syndromes. In Hoffman,R., Benz,E., Shattil,S., Furie,B., Cohen,H., Silberstein,L. and McGlave,P. (eds), *Hematology: Basic Principles and Practice*. Churchill Livingston, New York, NY, pp. 586–610.
17. Kang,S.H., Cho,M.J. and Kole,R. (1998) Up-regulation of luciferase gene expression with antisense oligonucleotides: implications and applications in functional assay development. *Biochemistry*, **37**, 6235–6239.
18. Jones,D.H. and Howard,B.H. (1991) A rapid method for recombination and site-specific mutagenesis by placing homologous ends on DNA using polymerase chain reaction. *Biotechniques*, **10**, 62–66.
19. Sierakowska,H., Sambade,M.J., Agrawal,S. and Kole,R. (1996) Repair of thalassemic human beta-globin mRNA in mammalian cells by antisense oligonucleotides. *Proc. Natl Acad. Sci. USA*, **93**, 12840–12844.
20. Stirchak,E.P., Summerton,J.E. and Weller,D.D. (1989) Uncharged stereoregular nucleic acid analogs: 2. Morpholino nucleoside oligomers with carbamate internucleoside linkages. *Nucleic Acids Res.*, **17**, 6129–6141.
21. Christensen,L., Fitzpatrick,R., Gildea,B., Petersen,K.H., Hansen,H.F., Koch,T., Egholm,M., Buchardt,O., Nielsen,P.E., Coull,J. *et al*. (1995) Solid-phase synthesis of peptide nucleic acids. *J. Pept. Sci.*, **1**, 175–183.
22. Koch,T., Hansen,H.F., Andersen,P., Larsen,T., Batz,H.G., Otteson,K. and Orum,H. (1997) Improvements in automated PNA synthesis using Boc/Z monomers. *J. Pept. Res.*, **49**, 80–88.
23. Kaiser,E., Colescott,R.L., Bossinger,C.D. and Cook,P.I. (1970) Color test for detection of free terminal amino groups in the solid-phase synthesis of peptides. *Anal. Biochem.*, **34**, 595–598.
24. Partridge,M., Vincent,A., Matthews,P., Puma,J., Stein,D. and Summerton,J. (1996) A simple method for delivering morpholino antisense oligos into the cytoplasm of cells. *Antisense Nucleic Acid Drug Dev.*, **6**, 169–175.
25. Schmajuk,G., Sierakowska,H. and Kole,R. (1999) Antisense oligonucleotides with different backbones. Modification of splicing pathways and efficacy of uptake. *J. Biol. Chem.*, **274**, 21783–21789.
26. Mercatante,D. and Kole,R. (2000) Modification of alternative splicing pathways as a potential approach to chemotherapy. *Pharmacol. Ther.*, **85**, 237–243.
27. Lacerra,G., Sierakowska,H., Carestia,C., Fucharoen,S., Summerton,J., Weller,D. and Kole,R. (2000) Restoration of hemoglobin A synthesis in erythroid cells from peripheral blood of thalassemic patients. *Proc. Natl Acad. Sci. USA*, **97**, 9591–9596.
28. Akhtar,S., Hughes,M.D., Khan,A., Bibby,M., Hussain,M., Nawaz,Q., Double,J. and Sayyed,P. (2000) The delivery of antisense therapeutics. *Adv. Drug Deliv. Rev.*, **44**, 3–21.
29. Bennett,C.F., Chiang,M.Y., Chan,H., Shoemaker,J.E. and Mirabelli,C.K. (1992) Cationic lipids enhance cellular uptake and activity of phosphorothioate antisense oligonucleotides. *Mol. Pharmacol.*, **41**, 1023–1033.
30. Condon,T.P. and Bennett,C.F. (1996) Altered mRNA splicing and inhibition of human E-selectin expression by an antisense oligonucleotide in human umbilical vein endothelial cells. *J. Biol. Chem.*, **271**, 30398–30403.
31. Karras,J.G., McKay,R.A., Dean,N.M. and Monia,B.P. (2000) Deletion of individual exons and induction of soluble murine interleukin-5 receptor-alpha chain expression through antisense oligonucleotide-mediated redirection of pre-mRNA splicing. *Mol. Pharmacol.*, **58**, 380–387.
32. Taylor,J.K., Zhang,Q.Q., Wyatt,J.R. and Dean,N.M. (1999) Induction of endogenous Bcl-xS through the control of Bcl-x pre-mRNA splicing by antisense oligonucleotides. *Nat. Biotechnol.*, **17**, 1097–1100.
33. Hodges,D. and Crooke,S.T. (1995) Inhibition of splicing of wild-type and mutated luciferase-adenovirus pre-mRNAs by antisense oligonucleotides. *Mol. Pharmacol.*, **48**, 905–918.
34. Kole,R. (1998) Modification of alternative splicing of pre-mRNA by antisense oligonucleotides. In Stein,C. and Krieg,A. (eds), *Applied Antisense Oligonucleotide Technology*. Wiley Liss Inc., New York, NY, pp. 451–469.
35. Schwarze,S.R., Hruska,K.A. and Dowdy,S.F. (2000) Protein transduction: unrestricted delivery into all cells? *Trends Cell. Biol.*, **10**, 290–295.
36. Lindgren,M., Gallet,X., Soomets,U., Hallbrink,M., Brakenhielm,E., Pooga,M., Brasseur,R. and Langel,U. (2000) Translocation properties of novel cell penetrating transportan and penetratin analogues. *Bioconjug. Chem.*, **11**, 619–626.
37. Derossi,D., Chassaing,G. and Prochiantz,A. (1998) Trojan peptides: the penetratin system for intracellular delivery. *Trends Cell. Biol.*, **8**, 84–87.
38. Lindgren,M., Hallbrink,M., Prochiantz,A. and Langel,U. (2000) Cell-penetrating peptides. *Trends Pharmacol. Sci.*, **21**, 99–103.